# ChemComm

Accepted Manuscript


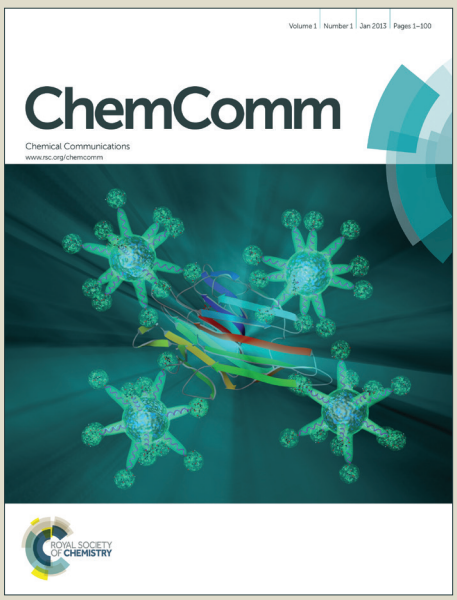





ROYAL SOCIETY OF CHEMISTRY

www.rsc.org/chemcomm

Cite this: DOI: 10.1039/c0xx00000x

www.rsc.org/xxxxxx

Communication

# A novel self-assembling nanoparticle of Ag/Bi with high reactive efficiency†

**Jianyu Gong,[a] Chung-Seop Lee,[a] Yoon-Young Chang[b] and Yoon-Seok Chang[a]***

***Received (in XXX, XXX) XthXXXXXXXXX 20XX, Accepted Xth XXXXXXXXX 20XX***

**DOI: 10.1039/b000000x**

**A novel Ag/Bi nanoparticle has been prepared *via* a facile precipitation approach. The nanoparticle could achieve purification of contaminated water without supplements and exhibited much higher activity than other popular nanoparticles (e.g. nZVI). The excellent performance of Ag/Bi was due in part to a large production of •OH radicals.**

Environmental problems associated with harmful water pollutants pose severe threats to human health. "Green" water treatment methods are considered most optimal, and are therefore the most often considered. Over the past decades, semiconductor photocatalysts, such as $TiO_2$, have received increasing attention because of their use in environmental pollution treatments under solar energy or visible light.[1] Often, the broad band gap of some photocatalysts limits the semiconductor use under solar light. As such, efforts have been made to address the inherent deficiency, using element doping, co-catalysts, morphology engineering, and others.[2] However, illumination requirements and complex semiconductor modifications limit the use of photocatalysts in real environments such as in river or in groundwater. Therefore, using another kind of nanoparticles with zero valence is an attractive option. Among these, nano-sized zero valent iron (nZVI or $Fe^0$) is the one that has been widely used in environmental purification without supplements.[3] Unfortunately the low redox potential and weak reaction activity of nZVI limits its use in purifying most normal recalcitrant organic compounds (such as phenol) that could not be treated or mineralized by nZVI alone. Therefore, a novel nanoparticle design is badly needed to replace traditional photocatalysts or nZVI nanoparticles in pollution abatement.

Recently, a series of new catalysts based on silver, such as $Ag_3PO_4$, $Ag_3AsO_4$, and $Ag_2O/Ag_2CO_3$,[4-6] have shown significantly higher activity than the other currently known photocatalysts because of the effect of $Ag^+$ inside the catalyst lattice. On the other hand, an interesting element, bismuth (Bi), has been considered as a candidate for Bi-based catalyst fabrication due to its excellent electronic properties and suitable conduction band.[7,8] For most Bi-based oxides (photocatalysts), the valence band (VB) is governed by O 2p and Bi 6s to narrow the band gap. Furthermore, the high catalytic activity of these materials are also ascribed to s composition in the VB because the photogenerated charge carriers in s orbital have a high mobility, caused by the dispersive property of Bi 6s orbital.[9]

In this study, we prepared a novel nanomaterial with zero chemical valence, Ag/Bi, through a facile precipitation process, easily treating phenol without any other supplements. Our study also investigated its crystalline structure, morphology, reactive activity, and degradation mechanism. To the best of our knowledge, this is the first report on Ag/Bi nanoparticles.

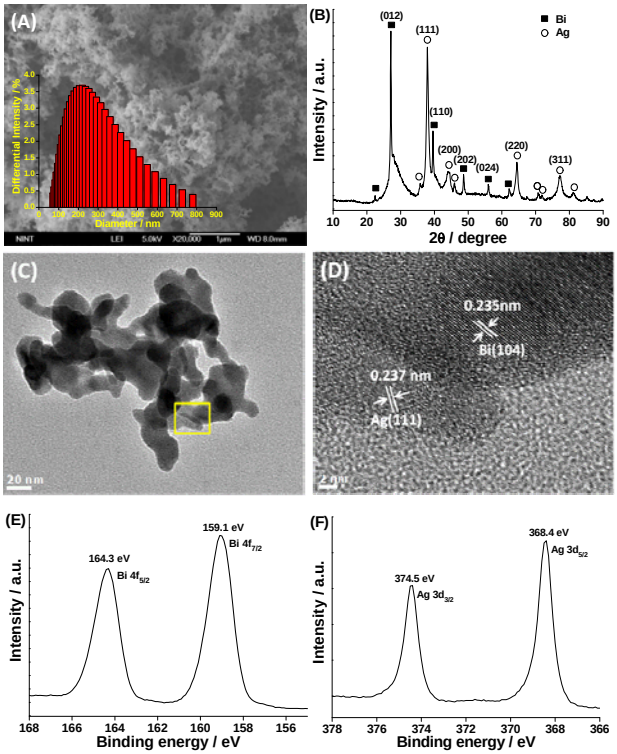


**Fig. 1** (A) SEM image, (B) XRD pattern, (C) TEM image, (D) HRTEM image and XPS spectra of (E) Bi 4f orbit and (F) Ag 3d orbit of Ag/Bi nanoparticles. The inset of (A) is the size distribution of Ag/Bi nanoparticles.

Fig. 1A presents a SEM image displaying the panoramic morphologies of the prepared particles. The image shows that the synthesized products are cotton-shaped with a main size distribution in the range of 150 ~ 220 nm (the inset of Fig. 1A) and have disordered mesoporosity between nanoparticles, confirmed by $N_2$ adsorption measurements (Fig. S1, ESI†). The nitrogen adsorption-desorption measurement results showed that

the BET surface area of Ag/Bi was approximately 8 $m^2/g$. This may be ascribed to the special porous structure of Bi, as shown in Fig. S2-A (ESI†), which significantly differs from the Ag structure (Fig. S2-B, ESI†). Fig. 1B shows the XRD pattern of the as-synthesized products. The diffraction peaks of Ag/Bi could be indexed to zero valent bismuth (JCPDS no. 010699) and zero valent silver (JCPDS no. 011167). No other peaks corresponding to bismuth oxides, silver oxides or other impurity phases were detected.

Fig. 1C shows the HRTEM image of the synthesized Ag/Bi, which is fully consistent with the SEM observations with respect to its morphologies and dimensionalities. The TEM images clearly demonstrate that the micro-net surface structure is an accumulation of many individual particles, with an average size of 20 nm. These sheets intersect with each other, resulting in the net-like morphology with porous structure. The porosity of the Ag/Bi nano-net was further confirmed by the clear lattice fringes shown in Fig. 1D and Fig. S3 (ESI†). The adjacent lattice planes correspond to the d-spacing of the Bi (104) and Ag (111) planes with spacing of 0.235 and 0.237 nm, respectively. The HRTEM images confirm that the synthesized Ag/Bi products have a highly crystalline structure, essential for high reactive activity. The elemental mapping analysis corresponding to the small area is shown in Figs. S4-A, B (ESI†), confirming the coexistence of Ag and Bi, which are evenly distributed in the Ag/Bi composite (Figs. S4-C and D, ESI†). Furthermore, the presence of Bi and Ag within the particles was also identified by the XPS global spectrum in Fig. S5 (ESI†). A trace amount of carbon in the spectrum was mainly attributed to the adventitious hydrocarbon from XPS itself.[10] Additionally, a small quantity of oxygen might be attributable to the exposure of Ag/Bi in room conditions.

Fig. 1E shows the high resolution XPS spectra of the Bi element. The peaks at 159.1 and 164.3 eV are associated with Bi $4f_{7/2}$ and Bi $4f_{5/2}$, respectively. The Ag 3d region (Fig. 1F) displays characteristic peaks at 368.4 and 374.5 eV, ascribed to the core levels of Ag $3d_{5/2}$ and Ag $3d_{3/2}$, respectively.

It is shown that the phenol degradation significantly depends on the mass ratio of Ag to Bi in Ag/Bi (Fig. 2A and Fig. S6, ESI†). An increase in the mass ratio from 0 to 0.5 correlates with an increase in phenol kinetic degradation ($k_{obs}$) from 0.114 $h^{-1}$ to 0.978 $h^{-1}$. However, while the mass ratio of Ag to Bi increases to 1.2, the $k_{obs}$ of phenol decreases to 0.378 $h^{-1}$. This may be due to the dual roles of Ag. On one hand, a higher Ag load will form a bimetallic structure with Bi, improving the reaction activity, because of fast electron transfer on the Ag surface. It will be discussed further below. On the other hand, since Ag can not dispose of the organic pollutant on its own, an even higher Ag load decreases the relative amount of Bi in the bimetallic nanoparticles, resulting in the lower degradation (see Fig. 2B). As such, we selected the mass ratio of 0.5 (Ag : Bi) in Ag/Bi as the best option for further study.

Fig. 2B shows the phenol degradation timeframes when exposed to different nanoparticles. Ag/Bi demonstrated much higher degradation efficiencies than the others. After 2 h of treatment, almost 100% phenol has been degraded by Ag/Bi. The phenol degradation rate with Ag/Bi was slightly improved in the presence of $O_2$. In the case of Bi alone, only 78% phenol was removed even after 4 h of treatment. On the other hand, there was only slight phenol degradation with nZVI (or Pd/ZVI),[11,12] widely used in pollution treatment.[3]

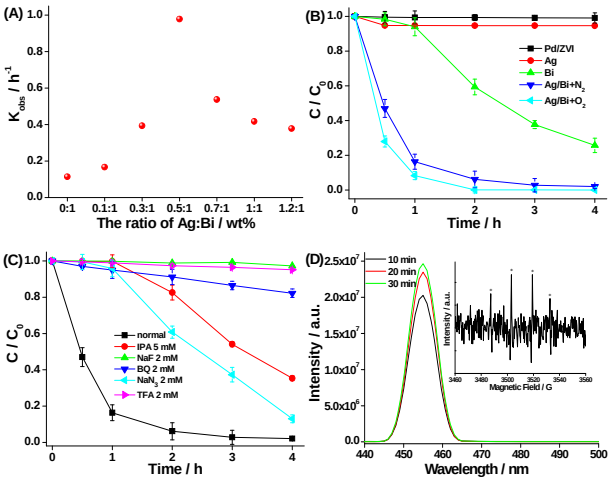


**Fig. 2** (A) Plot of the phenol degradation rate constants versus the different mass ratios of Ag to Bi in Ag/Bi nanoparticles, (B) comparison of phenol degradation by different nanoparticles, (C) effects of different scavenger conditions on the oxidative degradation of phenol by Ag/Bi, (D) fluorescence spectra of umbelliferone in 0.1 mM coumarin solutions in the presence of Ag/Bi. The inset is the ESR spectral signal of DMPO-•OH spin-trapping in water in the presence of Ag/Bi after 2 min of reaction. (DMPO = 50 mM, Ag/Bi = 1 g/L)

Next, we added a number of radical scavenging species to the combination of phenol with Ag/Bi, to determine the impact of intervention on degradation. These species included isopropanol (IPA), sodium fluoride (NaF), 1,4-benzoquinone (BQ), sodium azide ($NaN_3$), and trifluoroacetic acid (TFA). The goal was to investigate contributory roles of any reactive •OH generated in the solution (•$OH_{bulk}$), •OH radicals on the nanoparticles surface (•$OH_{ads}$), superoxide radical ($O_2$•$^-$), singlet oxygen ($^1O_2$), and electron ($e^-$).[13,14] Fig. 2C shows that, after 4 hours, the phenol concentration remains almost unchanged with the use of •$OH_{ads}$ radical scavenger (NaF) and electron radical scavenger (TFA), respectively. This suggests that the •$OH_{ads}$ and electrons are the dominant reactive species contributing to the oxidative phenol degradation with Ag/Bi. In addition, due to the residual of $O_2$ still remained in the phenol liquid even after purged with $N_2$, the phenol degradation efficiency decreased from 100% to 18% in the presence of $O_2$•$^-$ radical scavenger (BQ), implying that $O_2^{\bullet-}$ also played a role with Ag/Bi. It might explain the better efficiency of phenol degradation at highly dissolved $O_2$ concentrations, mentioned above (Fig. 2B). However, the phenol degradation efficiency decreased from 100% to 65% after 4h in the presence of IPA, indicating that •$OH_{bulk}$ might be generated a little in the system. When $NaN_3$ was added to the reaction, the degradation efficiency slightly decreased to 87% after 4h, proving that $^1O_2$ was not critical in the whole reaction process. Therefore, the •$OH_{ads}$ radical should be the most important oxidizing species during the reaction.

To further assess •$OH_{ads}$ radicals produced during the reaction process, coumarin (0.1 mM) was used to monitor these radicals in

the presence of Ag/Bi nanoparticles. Coumarin can react with •OH, forming highly fluorescent 7-hydroxycoumarin.[15] Fig. 2D shows that the increasing fluorescence intensities substantiate the production of $•OH_{ads}$ in the reactive process at the interface of Ag/Bi and water, which was also identified by the classical 1:2:2:1 spectral signal of spin trapped DMPO-•OH as shown in the inset of Fig. 2D. As far as we know, a portion of $•OH_{ads}$ is obtained by $O_2•^-$ which tends to transform into •OH in accordance with the following equations (1) and (2):

$$e^- + O_2 \rightarrow O_2•^- \quad (1)$$

$$O_2•^- + 2H_2O \rightarrow 2•OH + 2OH^- + O_2 \quad (2)$$

As such, the fluorescence spectra display might be due to the synthetic behavior of $O_2•^-$ and $•OH_{ads}$, resulting in the excellent degradation of phenol with Ag/Bi. Furthermore, the concentration of $•OH_{ads}$ generated by Ag/Bi is almost two times higher than by nZVI (Fig. S7, ESI†), which is good evidence to illustrate that phenol can be treated by Ag/Bi more effectively than nZVI.

The high activity of Ag/Bi nanoparticles is assumed to be the metallic $Ag^0$ and $Bi^0$ species formed during the initial stage of the degradation process. Metallic $Ag^0$ serves as an excellent electron acceptor and efficiently traps the electrons. In addition, due to the local electromagnetic field and excellent conductivity of the $Ag^0$ species, electrons are generated from the transformation of $Bi^0$ to $Bi^{3+}$ that can be transferred quickly to $Ag^0$.[16] The electrons trapped by the $Ag^0$ species further react with $H_2O$ or $O_2$ molecules adsorbed on the composite surface to form active $•OH_{ads}$ radicals, or directly involve in the degradation of phenol.

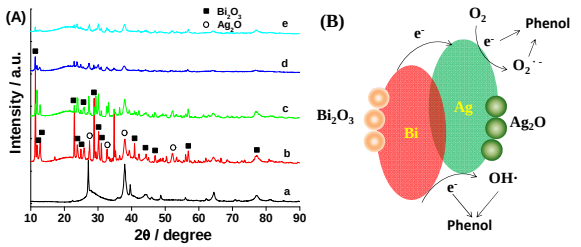


**Fig. 3** (A) XRD patterns of (a) fresh Ag/Bi and Ag/Bi after (b) 1, (c) 2, (d) 3, and (e) 4 h sequential exposures in phenol solutions and (B) suggested mechanism for the degradation of phenol by Ag/Bi.

For investigation of the Ag/Bi phase transformation during this reaction, Fig. 3A shows the XRD patterns of Ag/Bi after sequenced phenol treatments. In process of time, $Ag^0$ converts into $Ag_2O$ (JCPDS No.120793). Turning to $Bi^0$, the XRD patterns also show the $Bi_2O_3$ (JCPDS No. 710467) transformation. The standard reduction potentials of $Ag^0/Ag^+$ is +0.799 V and $Bi^0/Bi^{3+}$ is +0.308 V; therefore, the electron transfer from $Bi^0$ to $Ag^+$ ions is thermodynamically favored, as shown by:

$$Bi^0 + 3Ag^+ \rightarrow 3Ag^0 + Bi^{3+} \quad (3)$$

Most electrons generated from the transformation of $Bi^0$ to $Bi^{3+}$ are transfered to the surface of $Ag^0$, resulting in the fast phenol degradation by Ag/Bi. In addition, as shown in Fig. S8 (ESI†), the morphology of Ag/Bi also changes after the degradation reaction. Compared to the fresh Ag/Bi (Fig. 1A), piece-like composites formed in the used Ag/Bi nanoparticles. The EDX analysis (the inset of Fig. S8) shows that the piece-like composites (spectrum 1) are mainly formed by Bi atoms (9.93 at%), whereas the block-shape particles (spectrum 2) are mainly formed by Ag atoms (20.55 at%). Upon the basis of those experimental results, the schematic in Fig. 3B outlines the basis for the significantly enhanced activity of Ag/Bi.

## Conclusions

In this investigation, we successfully synthesized a novel highly reactive nanoparticle, Ag/Bi, through a facile precipitation approach. The newly developed Ag/Bi showed a zero valent chemical value. We then tested the reaction activity of Ag/Bi in phenol degradation, showing the complete removal efficiency resulting from its high concentration of $•OH_{ads}$ generated by Ag/Bi. This work presents an efficient nanoparticle that can be used to degrade persistent organic pollutants in wastewater without any other supplements. Furthermore, this new nanomaterial can also be applied to *ex-situ* oxidation treatments of contaminated groundwater, while nZVI has been more efficiently used in *in-situ* reductive remediation. The cost-effectiveness of this raw material was evaluated to compare with nZVI (ESI†). Although, considering the low toxicities of Ag[17] and Bi[18], the biocompatibility is expected not a problem, its nanotoxicity and mobility should be tested prior to the field application.

This work was supported by the National Research Foundation of Korea (NRF) grant funded by the Korea government (MEST) (No. 2011-0028723) and the GAIA project by the Korea Ministry of Environment.

## Notes and references

*a School of Environmental Science and Engineering, Pohang University of Science and Technology (POSTECH), Pohang, 790-784, Republic of Korea*
*b Department of Environmental Engineering, Kwangwoon University, Seoul, 139-701, Republic of Korea*
*Email: yschang@postech.ac.kr, Phone: +82-54-279-2281, Fax: +82-54-279-8299*

† Electronic Supplementary Information (ESI) available: [Experimental details, materials characterization and Figs. S1-S8]. See DOI: 10.1039/b000000x/

1 N. Liu, X. Y. Chen, J. L. Zhang and J. W. Schwank. *Catal. Today*, 2014, **225,** 34.
2 S. Ardo and G. J. Meyer. *Chem. Soc. Rev.*, 2009, **38,** 115.
3 W. J. Liu, T. T. Qian and H. Jiang, *Chem. Eng. J.* 2014, **236**, 448.
4 Z. G. Yi, J. H. Ye, N. Kikugawa, T. Kako, S. X. Ouyang, H. Stuart-Williams, H. Yang, J. Y. Cao, W. J. Luo, Z. S. Li, Y. Liu and R. L.Withers. *Nat. Mater.*, 2010, **9,** 559.
5 J. T. Tang, Y. H. Liu, H. Z. Li, Z. Tan and D. T. Li. *Chem. Commun.*, 2013, **49,** 5498.
6 C. L. Yu,G. Li, S. Kumar, K. Yang and R. C. Jin, *Adv. Mater.*, 2013, **26,** 892.
7 W.F. Su and Y.T. Lu, *Mater.Chem. Phys.*, 2003, **80,** 632.
8 S. L. Wang, W. H. Ma, Y. F. Fang, M. K. Jia and Y. P. Huang, *Appl. Catal., B* 2014, **150– 151,** 380.
9 J. W. Tang, Z. G. Zou and J. H. Ye, *J. Phys. Chem. C* 2007, **111**, 12779.
10 J.G. Yu and X.X. Yu, *Environ. Sci. Technol.*, 2008, **42,** 4902.
11 B. P. Chaplin, M. Reinhard, W. F. Schneider, C. Schüth, J. R. Shapley, T. J. Strathmann and C. J. Werth, *Environ. Sci. Technol.*, 2012, **46**, 3655.
12 J. H. Kim, P. G. Tratnyek and Y. S. Chang, *Environ. Sci. Technol.*, 2008, **42**, 4106.

13 L. Zhou, W. Song, Z. Q. Chen and G. C. Yin,*Environ. Sci. Technol.*, 2013, **47,** 3833.
14 H.Hori, A. Yamamoto, K. Koike, S. Kutsuna, M. Murayama,A. Yoshimoto and R.Arakawa, *Appl. Catal., B* 2008, **82,** 58.
15 K. Ishibashi, A. Fujishima, T. Watanable and K. Hashimoto, *Electrochem. Commun.,* 2000, **2,** 207.
16 D. W. Wang, Y. Li, G. L. Puma, C. Wang, P. F. Wang, W. L. Zhang and Q. Wang, *Chem. Commun.,* 2013, **49,** 10367.
17 S. Eckhardt, P. S. Brunetto, J. Gagnon, M. Priebe, B. Giese and K. M. Fromm, *Chem. Rev.,* 2013, **113**, 4708.
18 R. Mohan, *Nature Chemistry,* 2010, **2**, 336.